Magnetic properties of Cu-doped GaN grown by molecular beam epitaxy

Philipp R. Ganz,[1,2] Gerda Fischer,[3] Christoph Sürgers,[1,3,*] and Daniel M. Schaadt[1,2,4]

[1]*Karlsruhe Institute of Technology, DFG-Center for Functional Nanostructures, P.O. Box 6980, 76049 Karlsruhe, Germany*
[2]*Karlsruhe Institute of Technology, Institut für Angewandte Physik, P.O. Box 6980, 76049 Karlsruhe, Germany*
[3]*Karlsruhe Institute of Technology, Physikalisches Institut, P.O. Box 6980, 76049 Karlsruhe, Germany*
[4]*Clausthal University of Technology, Institute for Energy Research and Physical Technologies, Am Stollen 19B, 38640 Goslar, Germany*

(Received 6 June 2011; revised manuscript received 31 January 2012; published 5 April 2012)

Cu-doped GaN films were epitaxially grown by molecular beam epitaxy on *C*-plane sapphire substrates with an AlN buffer layer. Growth under metal-rich and nitrogen-rich conditions was investigated for different Cu-to-Ga beam-equivalent-pressure ratios x_{BEP}. The samples were characterized by scanning electron microscopy, energy dispersive x-ray spectroscopy, and x-ray diffraction. Films within a narrow range of x_{BEP} around 1% exhibit ferromagnetic behavior with a Curie temperature higher than 400 K. For higher $x_{\mathrm{BEP}} > 1\%$, islands of a Cu-Ga compound are predominantly formed at the surface as nonferromagnetic precipitates. Our detailed study shows that the saturation magnetization of ferromagnetic films with $x_{\mathrm{BEP}} \approx 1\%$ decreases with increasing film thickness. This suggests that the ferromagnetism arises from defects, such as threading dislocations, created by the incorporation of Cu into the GaN.

DOI: 10.1103/PhysRevB.85.165204 PACS number(s): 75.70.Ak, 75.50.Pp, 68.55.ag, 81.15.Hi

I. INTRODUCTION

Over the last years, dilute magnetic semiconductors (DMSs) have been proposed to show ferromagnetism at room temperature.[1,2] This has stimulated considerable interest in view of their possible applications in spintronic devices.[3] Among the various semiconductors that are candidates for DMSs, group III nitrides are attractive for optoelectronic applications and devices due to their large band gap and their thermal and chemical stability. In particular, GaN is the best characterized group III nitride. Investigations to probe possible ferromagnetism in DMSs usually focus on doping with transition metals. Indeed, ferromagnetism at room temperature was predicted and observed for Mn- and Gd-doped GaN.[1,2,4–6] However, the origin of ferromagnetism in these materials is still under debate, because Mn and Gd are intrinsic magnetic elements and tend to form clusters or precipitates in the GaN host which may also cause the observed ferromagnetic behavior.[7,8]

In order to unambiguously attribute the origin of ferromagnetism to an intrinsic property of the DMS and to avoid formation of ferromagnetic transition-metal precipitates, the use of a dopant that as a precipitate is nonmagnetic, like Cu, is more favorable. Previously, ferromagnetism was reported to occur in Cu-doped ZnO.[9,10] ZnO and GaN are semiconductors that solidify in the wurtzite structure with similar lattice constants and direct band gaps. Hence, Cu might also serve as an appropriate dopant to induce ferromagnetic order in GaN. However, possible ferromagnetic order in Cu-doped GaN has been discussed controversially by theory. Wu *et al.* proposed a ferromagnetic ground state with 100% spin polarization, a magnetization of 2.0 μ_{B} per Cu atom, and a Curie temperature of 350 K.[11] In contrast, Rosa *et al.* expect a rather weak ferromagnetism inferred from density-functional-theory (DFT) calculations.[12] The latter suggests that the substituted Cu atom prefers to be separated from the next Cu neighbor by only a short distance and the associated relaxation of the Cu-N-Cu bond angle causes a significant decrease of the magnetic moments of Cu and N.

Room-temperature ferromagnetism was experimentally observed in GaN calcined with CuO in nitrogen flux[13] and in Cu^{+}-ion-implanted GaN[14,15] with a magnetic moment $\mu = 0.01$–0.27 $\mu_{\mathrm{B}}/\mathrm{Cu}$ much smaller than predicted.[11] For Cu-implanted GaN, μ depends crucially on the annealing conditions. This indicates that defects, introduced into the GaN lattice during ion implantation, play an important role concerning the saturation magnetization. A larger magnetic moment of 0.86 $\mu_{\mathrm{B}}/\mathrm{Cu}$ was observed in Cu-doped GaN nanowires.[16] DFT calculations predict that Cu tends to substitute Ga inside the nanowire, resulting in an enhanced ferromagnetic stability compared to the bulk.[17]

In light of potential applications, epitaxial growth of Cu-doped GaN films by molecular beam epitaxy (MBE) is indispensable. First investigations on Cu-doped GaN grown by hybrid physical-chemical vapor deposition and MBE have been published recently.[18,19] Here, we report the characterization and magnetic properties of epitaxial Cu-doped GaN films grown by activated N_2-plasma-assisted MBE from individual Cu and Ga sources under metal-rich and nitrogen-rich growth conditions. Films with a Cu-to-Ga beam-equivalent pressure (BEP) ratio $x_{\mathrm{BEP}} \approx 1\%$ show ferromagnetic behavior with a Curie temperature $T_{\mathrm{C}} > 400$ K and a saturation magnetization that strongly depends on the thickness of the GaN:Cu film.

II. EXPERIMENT

Cu-doped GaN was grown by plasma-assisted MBE on (0001)-oriented *C*-plane sapphire substrates using three effusion cells for Al (purity 99.9999%), Ga (purity 99.99999%), and Cu (purity 99.9999%). The substrates were glued with indium (purity 99.999%) onto silicon wafers to provide good thermal contact to the heated substrate holder. An AlN seed layer (wurtzite structure) of ≈5 nm thickness was formed on Al_2O_3 by nitridation of the sapphire surface at a substrate temperature $T_{\mathrm{S}} = 200\,^{\circ}\mathrm{C}$ in a constant nitrogen partial pressure of 3.2×10^{-5} Pa with about 1.0% activated nitrogen N_2^{*}. After nitridation, a 20-nm-thick AlN buffer layer was deposited under Al-rich conditions to further reduce the lattice mismatch

 ©2012 American Physical Society

TABLE I. Sample parameters of GaN:Cu grown on (0001)-oriented C-plane sapphire with a 20-nm AlN buffer layer. V_{GaN}, GaN volume; m_S, magnetic moment measured at $\mu_0 H = 0.2$ T after subtraction of the diamagnetic background; M_S, saturation magnetization $M_S = m_S/V_{\mathrm{GaN}}$.

Sample No.	Growth mode	x_{BEP} (%)	d_{GaN} (nm)	V_{GaN} (10^{-6} cm^3)	m_S (10^{-9}A m^2)	M_S (10^3A/m)
N0300	Metal rich	0	140	10.15	20	2.0
N0304	Metal rich	0.1	140	11.06	7	0.63
N0303	Metal rich	0.4	140	10.50	5	0.48
N0332[a]	Metal rich	0.9	180	11.97	70	5.85
N0362	Metal rich	1.1	60	4.14	43.6	10.53
N0363	Metal rich	1.1	400	28.0	1.7	0.06
N0121	Metal rich	1.2	140	3.36	17	5.06
N0301	Metal rich	1.2	140	11.27	28	2.48
N0356	Metal rich	2.1	180	17.28	19	1.10
N0192	Metal rich	2.8	140	10.31	26	2.52
N0140	Metal rich	4.8	280	13.86	23.5	1.70
N0336	N rich	0.7	80	5.67	24	4.23
N0348	N rich	0.9	240	17.83	30	1.68
N0364[b]	N rich	1.1	60	7.25	17	5.35
N0335	N rich	1.1	100	7.91	68	8.60
N0354	N rich	1.1	360	29.52	21	0.71
N0334	N rich	1.3	85	5.95	27	4.53
N0217	Cu-Ga film	100	132	9.90	15	1.52
N0358	Cu-Ga film in N_2	100	100	7.25	9.5	1.31

[a]Highly metal-rich growth.
[b]Grown on a 5-μm GaN template without AlN buffer layer.

between GaN and sapphire to ≈3.9%. Subsequently, Cu-doped GaN was grown at $T_S = 790\,^\circ$C (thermocouple reading) from individual Cu and Ga sources. Throughout this paper the nominal doping level is given by the BEP ratio x_{BEP}. The BEP ratio is usually different from the atomic concentration x of Cu dopands incorporated in the GaN film.[20] x depends on the temperature-dependent sticking coefficients and incorporation probabilities of all three constituents. Hence, the BEP ratio gives an upper limit for the Cu doping level.

Samples with thickness $d_{\mathrm{GaN}} = 60$–400 nm were grown under metal-rich (nitrogen-rich) conditions with a growth rate of 65 nm/h (45 nm/h) and a Ga/N_2^* ratio of 1.1 (0.8). For investigating the effect of Cu-Ga islands formed at the surface (see below) on the magnetic properties, two samples with $x_{\mathrm{BEP}} = 100\%$ were grown either without (sample N0217) or in N_2 atmosphere with a Ga/N_2 ratio of 1.1 (sample N0358). In addition, one GaN film was grown on a 5-μm-thick GaN template without an AlN buffer (sample N0364) for comparison. Table I shows the parameters of all samples investigated in this study.

The crystalline quality of the samples was checked by x-ray diffraction (XRD) in a four-circle diffractometer (D8 Discover, Bruker AXS) using filtered Cu $K_{\alpha 1}$ radiation and a fourfold Ge (022) monochromator. The surface morphology was investigated by atomic-force microscopy (AFM) in noncontact mode, scanning electron microscopy (SEM), and by energy dispersive x-ray spectroscopy (EDX) with an excitation energy of 10 keV.

The magnetization M of the samples was measured by means of a superconducting quantum-interference device (SQUID) magnetometer between 10 K and 400 K with the magnetic field oriented parallel to the film plane. For this purpose, one to three pieces ($\sim 5 \times 5$ mm^2 each) were fixed into a plastic straw serving as a sample holder. Magnetically active defects in the plastic straw gave rise to a small contribution of $\sim 5 \times 10^{-9}$ A m^2 to the total measured moment, which is of the size of the accuracy 3×10^{-9} A m^2 of our measurement (see below).

III. CHARACTERIZATION

A. Metal-rich growth

Figure 1 shows SEM images of (a) an undoped GaN film and of three samples with varying BEP ratios (b) 1.2%, (c) 2.0%, and (d) 4.8%. The surface of the Cu-doped samples

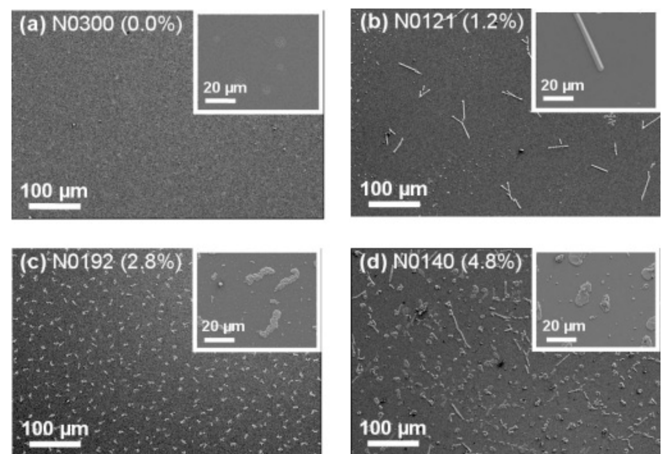

FIG. 1. SEM images of the samples with varying BEP ratio. The insets show images with a higher magnification.

is covered by laterally separated islands in contrast to the undoped film. The uncovered part of the surface has an average roughness of 0.8–1.6 nm determined from AFM topographs. With increasing BEP ratio, the number of large islands as well as the overall island volume increases while the number of small islands decreases. Figure 1(b) shows several small islands with an average diameter of 2 μm and only a few larger islands of needlelike shape while for the larger BEP ratio shown in Fig. 1(d) the surface is covered by larger islands with an average size of 10×15 μm^2. This is due to the decisive roles of different adatom mobilities and sticking coefficients S ($S_{Cu} \approx 1$, $S_{Cu} \ll 1$) on the kinetics of the growing film.[20]

The composition of the islands was investigated by EDX. Figure 2 shows spectra taken on sample N0121 with the incident electron beam focused on (a) an island and (b) on the uncovered surface of the epitaxial film. Peaks resolved in the spectra of the island (a) are attributed to the Cu L edge ($E = 0.95$ keV), Cu K edge ($E = 8.04$ keV), Ga L edge ($E = 1.11$ keV), and N K edge ($E = 0.392$ keV). On the uncovered part of the epitaxial layer a Cu signal was not observed within the detection limit (1–2 at. %) of the EDX setup, see Fig. 2(b). The additional peak measured at $E = 1.5$ keV is attributed to the Al K edge arising from the AlN buffer layer and the Al_2O_3 substrate. In addition, the intensity of the N K line has increased. The Al peak was not observed in Fig. 2(a) due to the attenuation by the

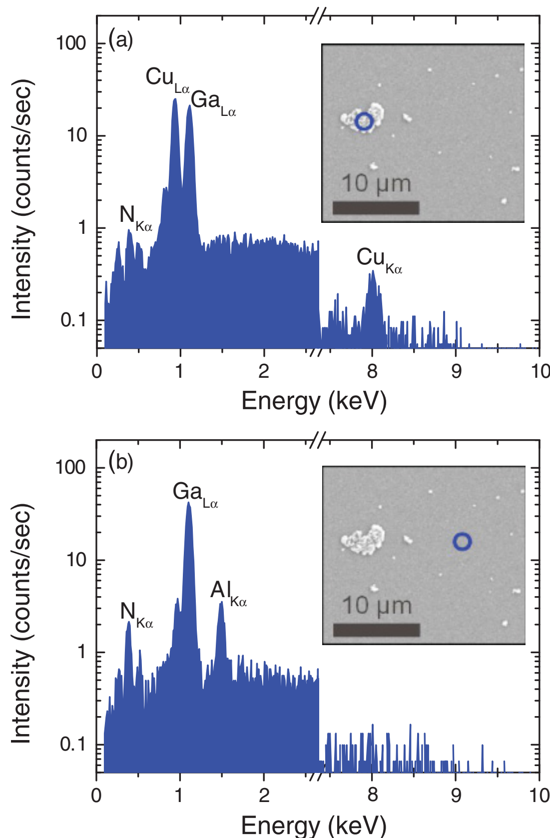

FIG. 2. (Color online) EDX spectra metal-rich grown GaN:Cu ($x_{BEP} = 1.2\%$, sample N0121) taken with the electron beam focused on (a) an island and (b) the uncovered epitaxial film. The point of focus is marked by a circle in the corresponding SEM images (insets).

200-nm-thick island where the thickness was determined by AFM. Similar results were obtained for a higher excitation energy of 15 keV. From the peak-to-peak ratios of the L edges a composition of $Cu_{0.6}Ga_{0.4}$ in the island was estimated taking into account similar sensitivity factors for Ga and Cu.

The question is what compound is formed in the islands? According to the thermodynamic phase diagram of binary Cu-Ga alloys, only $CuGa_2$, Cu_3Ga, and Cu_9Ga_4 appear to be stable.[21] These compounds are difficult to remove by wet chemical etching. We tried to reduce the number of islands by etching in a 30 vol % HCl solution for 10 min. Afterward, the islands were still observed by SEM but with fringed edges. Additional etching with 65 vol % HNO_3 solution for 5 min was also unable to completely remove the islands. This chemical resistance is presumably due to the formation of a GaN layer covering the islands. Indeed, cross-sectional TEM investigations together with EDX and wavelength-dispersive x-ray spectroscopy (WDX) indicate that the islands are composed of cubic Cu_9Ga_4—with in-plane orientations $Cu_9Ga_4[111] \parallel$ GaN$[1\bar{2}10]$ and $Cu_9Ga_4(10\bar{1}) \parallel$ GaN(0001)—and are partially covered by GaN.[22] The stoichiometric composition of Cu_9Ga_4 corresponds to $Cu_{0.69}Ga_{0.31}$, which is in reasonable agreement with $Cu_{0.6}Ga_{0.4}$ inferred from the EDX spectra reported here and in Ref. 22. The cross-section TEM images also show that no other secondary phases than Cu_9Ga_4 are formed.

XRD was employed to check for the crystalline quality of the samples. Figure 3(a) shows a $\theta - 2\theta$ scan for the as-grown 1.2% Cu-doped GaN (sample N0121). Bragg reflections arising from the GaN host, AlN buffer layer, and Al_2O_3 substrate are indexed according to the hexagonal structure. The full width at half maximum (FWHM) $\Delta\omega = 0.047^\circ$ of the GaN (0002) rocking curve [Fig. 3(a), inset] indicates very good epitaxial growth along the hexagonal c axis of GaN. In addition, two peaks observed at 22.2° and 49.8° are attributed to the formation of Cu_9Ga_4. Figure 3(b) shows the XRD scan of the same sample recorded after etching in HNO_3 for 5 min. The Cu-Ga peak at 49.8° disappeared completely and the intensity of the peak at 22.2° is strongly reduced. On the undoped GaN film N0300 no contributions from a Cu-Ga compound were observed [see Fig. 3(c)]. This confirms that the islands on the surface of Cu-doped GaN observed by SEM (Fig. 1) are due to Cu_9Ga_4.

B. Nitrogen-rich growth

Samples grown under N-rich conditions were characterized accordingly. Figure 4(a) shows a SEM image of sample N0335. The bright part of the surface has an average roughness of 3.1 nm obtained from an AFM topograph (not shown). This bright "background" is due to an incoherent or columnarlike growth of GaN under N-rich conditions, in contrast to metal-rich grown GaN. Dark circular regions originate from initial nucleation of Ga droplets on the AlN buffer layer at the early stages of GaN growth. The Ga droplets are consumed during subsequent growth of densely packed GaN providing a darker contrast in SEM. The average volume of the islands and their areal density is smaller for N-rich than for metal-rich grown samples.

The islands located in the center of the dark regions on the surface are identified as Cu_9Ga_4-like for the metal-rich

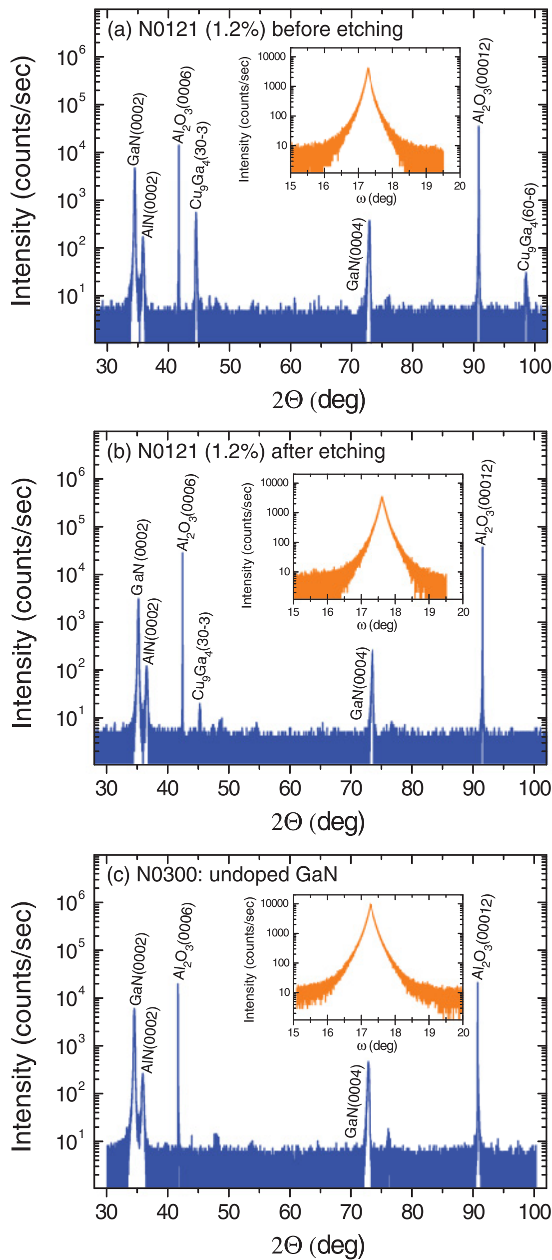

FIG. 3. (Color online) X-ray diffraction diagrams ($\theta - 2\theta$ scans) for metal-rich grown Cu-doped GaN ($x_{\mathrm{BEP}} = 1.2\%$, sample N0121) (a) before and (b) after etching with HNO_3 for 5 min. (c) X-ray diffraction diagram of undoped GaN film N0300. The insets show rocking curves (ω scans) of the GaN(0002) reflection. Intensity is always in logarithmic scale.

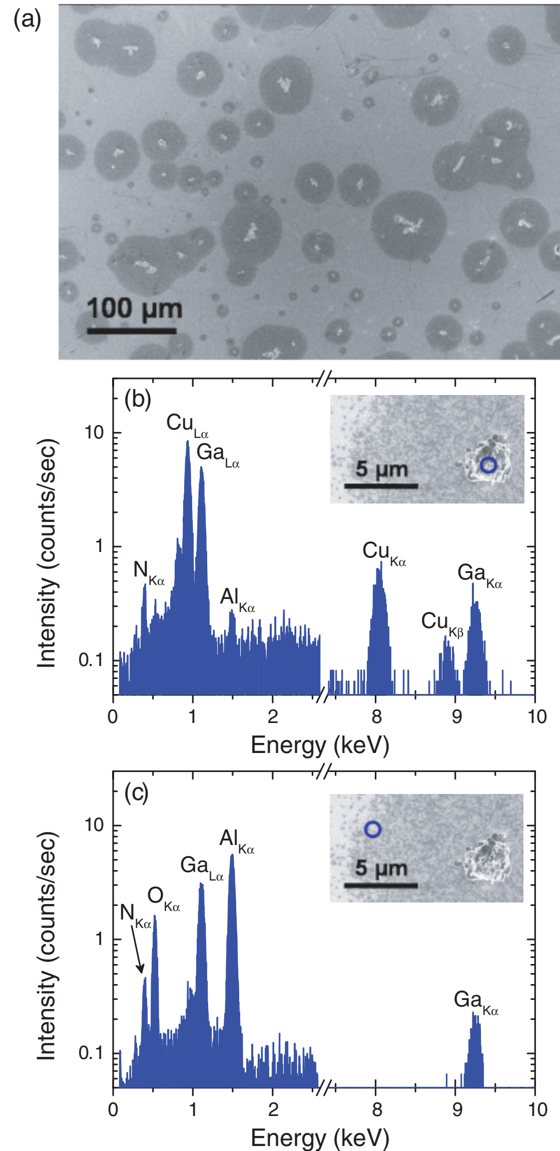

FIG. 4. (Color online) N-rich grown Cu-doped GaN ($x_{\mathrm{BEP}} = 1.1\%$, sample N0335). (a) SEM image. (b),(c) EDX spectra taken with the electron beam focused on (b) an island and (c) the uncovered GaN surface. The insets show SEM images where the point of focus is marked by a circle.

grown samples. This is confirmed by the EDX spectra shown in Figs. 4(b) and 4(c) obtained with the incident beam focused on (b) an island and (c) on the uncovered GaN surface. From the Cu-to-Ga peak ratio a composition $Cu_{0.62}Ga_{0.38}$ was estimated in good agreement with the stoichiometry of Cu_9Ga_4. The large peak arising from oxygen in Fig. 4(c) was not observed for samples grown under metal-rich conditions (cf. Fig. 2). In the N-rich grown sample this is attributed to oxygen from the Al_2O_3 substrate, which is seen by the EDX system due to the columnarlike growth, and a smaller GaN film thickness.

The crystalline quality of these samples is similar to samples grown under metal-rich conditions as determined from the XRD diagrams (Fig. 5), albeit a broader GaN (0002) rocking curve with a FWHM $\Delta\omega = 0.184^\circ$ was measured.

IV. MAGNETIC PROPERTIES

A. Magnetization of as-grown GaN:Cu samples

Magnetization measurements were performed on as-grown (nonetched) samples. Since the magnetic moment of the thin GaN:Cu film was generally weak, we first describe our routine to determine the magnetization of GaN:Cu. Figure 6(a) shows the magnetic moment $m(H)$ of a sapphire substrate (volume $V_{\mathrm{sub}} = 31.68$ mm^3) at $T = 10$ K. The negative slope is due to the diamagnetic response of the Al_2O_3 substrate. From

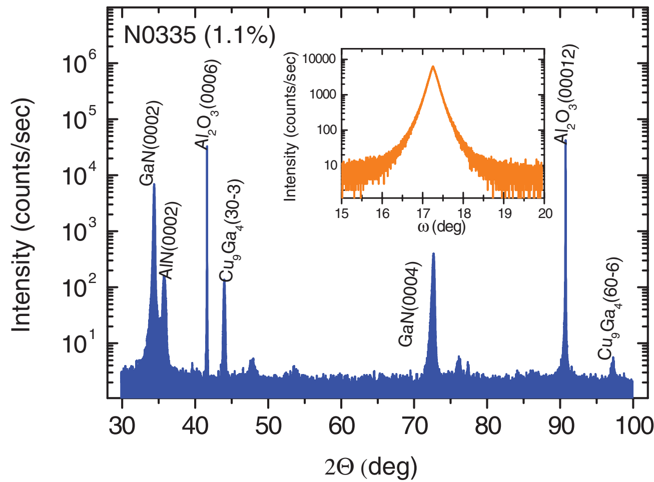

FIG. 5. (Color online) X-ray diffraction diagram ($\theta - 2\theta$ scan) of N-rich grown Cu-doped GaN ($x_{\mathrm{BEP}} = 1.1\%$, sample N0335). The inset shows the rocking curve (ω scan) of the GaN(0002) reflection.

the slope dm/dH of the linear fit to the data we obtain a magnetic susceptibility $\chi = (dm/dH)/V_{\mathrm{sub}} = -16.17 \times 10^{-6}$ (SI units) at $T = 10$ K and $\chi = -16.26 \times 10^{-6}$ at $T = 290$ K. Both values are in very good agreement with $\chi(10\,\mathrm{K}) = -16.1 \times 10^{-6}$ and $\chi(300\,\mathrm{K}) = -16.8 \times 10^{-6}$ reported earlier.[23] In Fig. 6(b) the total moment of sample N0332 with $x_{\mathrm{BEP}} = 0.9\%$ is plotted (open symbols). From

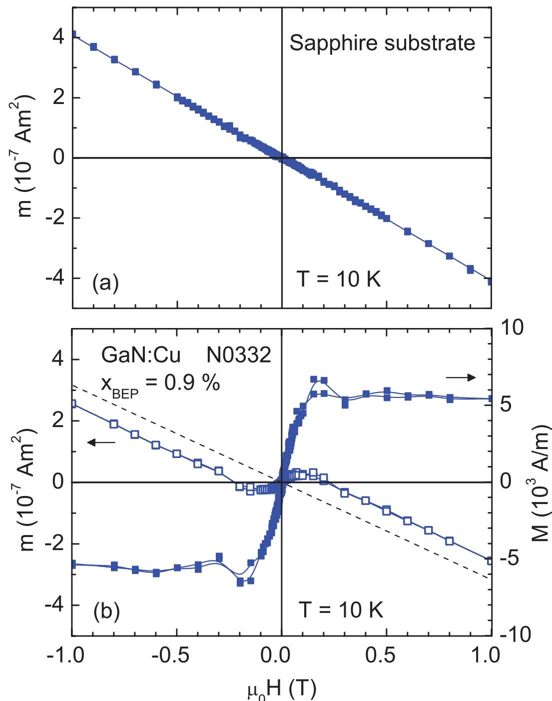

FIG. 6. (Color online) (a) Magnetic moment m vs magnetic field H of a sapphire substrate at $T = 10$ K. (b) Magnetization curve of GaN:Cu ($x_{\mathrm{BEP}} = 0.9\%$, sample N0332) at $T = 10$ K. Open symbols, magnetic moment $m(H)$ of GaN:Cu and substrate (raw data). Dashed line indicates the diamagnetic contribution of the sapphire substrate. Closed symbols, magnetization $M(H)$ of GaN:Cu after subtraction of the substrate contribution to m.

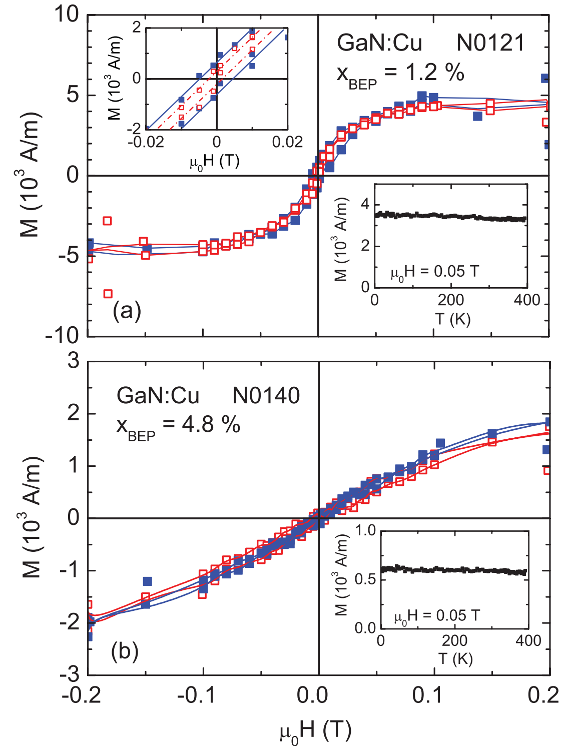

FIG. 7. (Color online) Magnetization curves of GaN:Cu films with (a) $x_{\mathrm{BEP}} = 1.2\%$ and (b) $x_{\mathrm{BEP}} = 4.8\%$ measured at $T = 10$ K (solid symbols) and at 290 K (open symbols). Bottom-right insets show the temperature dependence $M(T)$ measured in a field $\mu_0 H = 0.05$ T. Top left inset in (a) shows $M(H)$ close to zero field.

a fit to the data in the linear regime of $m(H)$ we determine $\chi(10\,\mathrm{K}) = -16.7 \times 10^{-6}$ (dashed line) in good agreement with χ of the pure sapphire substrate. The magnetization $M(H) = [m(H) - \chi V_{\mathrm{sub}} H]/V_{\mathrm{GaN}}$ of GaN:Cu is shown in Fig. 6(b) (solid symbols) with a saturation magnetization $M_{\mathrm{S}} = 5.85 \times 10^3$ A/m. V_{GaN} is the volume of the GaN:Cu film determined from the thickness d_{GaN} and the surface area of the GaN:Cu film. Table I shows the M_{S} values of all investigated samples.

Figure 7 displays magnetization curves $M(H)$ of two samples with higher x_{BEP} measured at $T = 10$ K and at $T = 290$ K. Sample N0121 exhibits a similar hysteresis like sample N0332 [cf. Fig. 6(b)] with a saturation at $\approx$0.1 T. At 10 K, a coercivity of $\approx$5 mT is estimated [Fig. 7(a), inset] which decreases to $\approx$2 mT at 300 K. Sample N0140 with a considerable higher $x_{\mathrm{BEP}} = 4.8\%$ is harder to saturate [see Fig. 7(b)]. Temperature has only little effect on the magnetization $M(H)$, as inferred from $M(T)$ of both samples measured between 10 K and 400 K in a field of 0.05 T (see insets of Fig. 7). $M(T)$ decreases only by 5%–7% between 10 K and 400 K indicating a Curie temperature $T_{\mathrm{C}} \gg 400$ K.

Samples N0121 and N0140 were additionally measured with the magnetic field oriented perpendicularly to the film plane to check for a possible out-of-plane component of the magnetization. However, no magnetic hysteresis curve was obtained in those cases.

Values of the saturation magnetization M_{S} determined in a magnetic field of 0.2 T at $T = 10$ K are plotted vs x_{BEP} in Fig. 8(a). $M_{\mathrm{S}}(x_{\mathrm{BEP}})$ shows a maximum of $\approx 10^4$ A/m in a

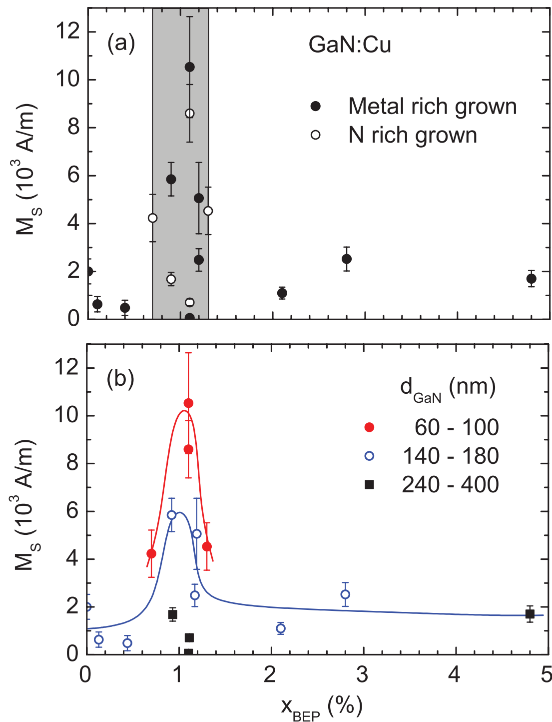

FIG. 8. (Color online) (a) Saturation magnetization of GaN:Cu at $T = 10$ K vs BEP ratio x_{BEP} for samples grown under different conditions (see Table I). The gray area indicates the range $x_{BEP} \approx 1\%$, where M_S is enhanced. (b) Same data as (a) but classified into three thickness ranges. Solid lines serve as guides to the eye.

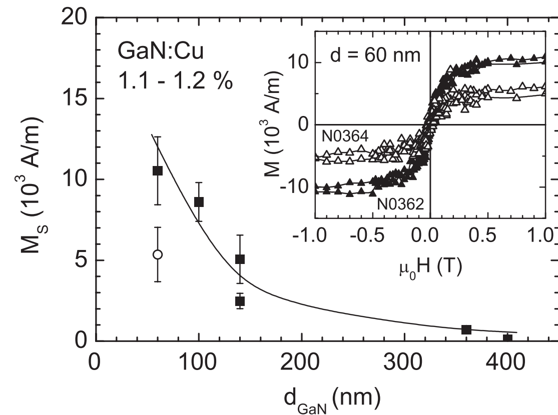

FIG. 9. Saturation magnetization of GaN:Cu films with $x_{BEP} = 1.1$–1.2% at $T = 10$ K vs thickness d_{GaN}. The open circle indicates sample N0364. The solid line serves as a guide to the eye. The inset shows $M(H)$ of two 60-nm-thick samples with $x_{BEP} = 1.1\%$ grown on 20-nm Al buffer layer (solid triangles, N0362) and on a 5-μm-thick GaN template (open triangles, N0364).

narrow range of doping levels close to $x_{BEP} = 1\%$. Samples with x_{BEP} outside this narrow range have a much lower $M_S \approx 1.5-2 \times 10^3$ A/m. The increase of M_S around $x_{BEP} = 1\%$ appears to be independent of the growth conditions, that is, metal-rich or N-rich growth. However, the absolute values vary strongly between almost zero and 10^4 A/m. This variation is resolved if the samples are classified into three sets of thickness $d_{GaN} = 60$–100 nm, 140–180 nm, and 240–400 nm. Figure 8(b) clearly shows that the maximum of M_S decreases with increasing thickness, suggesting an influence of the structural quality, that is, defect density, of the film. In heteroepitaxy, defects are generated in the growing film to reduce the misfit strain between substrate and film. It has been demonstrated that 20%–40% of the defects in MBE-grown GaN films are threading dislocations.[24] The dislocations provide current leakage paths which are the dominant source of leakage current in Schottky contacts to n-type GaN grown by MBE.[25]

The dependence of M_S on the film thickness is shown in Fig. 9 for six samples with almost the same $x_{BEP} = 1.1\%$–1.2%. This thickness dependence cannot be explained by a magnetization arising from secondary phases or precipitates in the bulk of the film as reported earlier, for instance, in (Ga,Mn)N.[8] A further proof of the influence of the structural quality on M_S is obtained from the comparison of GaN:Cu films prepared with the same parameters $x_{BEP} = 1.1\%$ and $d_{GaN} = 60$ nm but grown on 20-nm AlN buffer (N0362) and on a 5-μm-thick GaN template (N0364) without AlN buffer. Qualitatively, a strongly reduced defect density and reduced M_S are expected for the GaN:Cu film grown on GaN compared to AlN. Indeed, we observe a decrease of M_S by 50% (see the open circle in Fig. 9 and data in the inset). This is in agreement with preliminary measurements of the dislocation density at the surface of our GaN:Cu films by etch-pit decoration,[25] which indicate a factor of two larger dislocation density for the 60-nm-thin film N0362 than for the 400-nm-thick film N0363.

B. Role of Cu-Ga islands

In order to investigate the magnetic properties of Cu-Ga islands, we intentionally deposited two Cu-Ga films with $x_{BEP} = 100\%$ on top of an undoped GaN film at a low $T_S = 650$ °C without N_2 (sample N0217) and at $T_S = 500$ °C in N_2 atmosphere (sample N0358) (see Table I). Both samples showed a similar behavior like the undoped GaN film (N0300) with $M_S = 1.3-1.5 \times 10^3$ A/m much lower than the M_S values for samples with $x_{BEP} \approx 1\%$. Moreover, Cu-N compounds such as Cu_3N decompose at temperatures 330 °C–340 °C[26] much lower than the substrate temperatures T_S used in this study.

As already mentioned in Sec. III, etching the samples in HCl and HNO_3 does not remove the Cu-Ga islands completely. However, wet chemical etching might change the sample microstructure by dissolution of metal precipitates and/or remove magnetic impurities from the surface. For instance, etch-pit decoration of the n-type GaN surface is caused by a chemical modification confined to the immediate vicinity of each dislocation providing a conduction path.[25,27]

Figure 10 shows magnetization curves of three samples before and after etching in HCl for 4 min. In each case, the magnetization is reduced after etching, even for the undoped GaN film $x_{BEP} = 0$. We only mention that a second etching step in HNO_3 did not change the $M(H)$ behavior further. Since the etching reduces M_S of the undoped GaN film, too [cf. Fig. 10(a)], and the intentionally grown Cu-Ga films do not exibit an enhanced M_S we conclude the ferromagnetic behavior in MBE-grown GaN:Cu cannot arise from Cu-Ga islands. Moreover, a ferromagnetic Cu-Ga compound as well

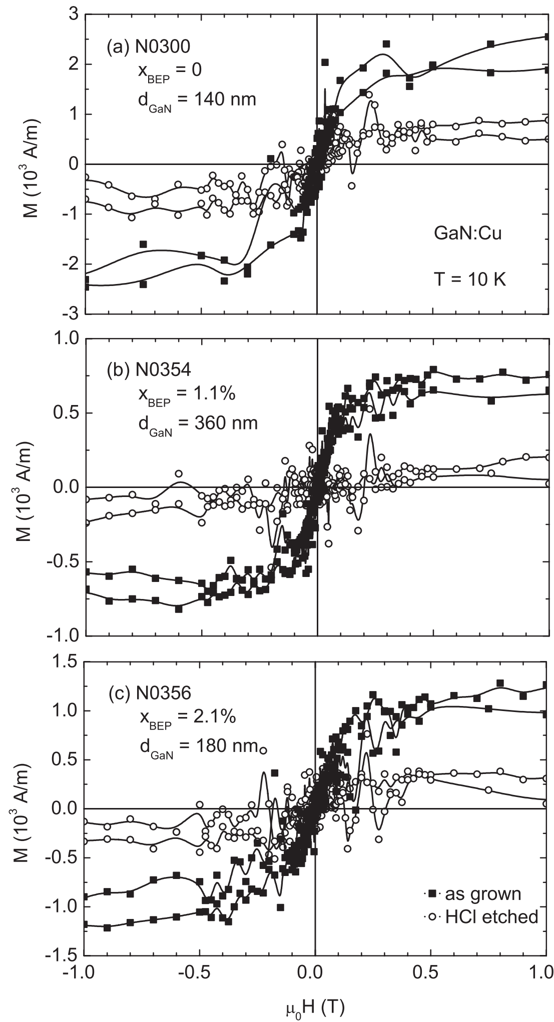

FIG. 10. $M(H)$ at $T = 10$ K of GaN:Cu films of different BEP ratios (a) $x_{\text{BEP}} = 0$, (b) $x_{\text{BEP}} = 1.1\%$, and (c) $x_{\text{BEP}} = 2.1\%$ as grown (solid squares) and after etching in HCl (open circles).

as magnetic impurities at the surface or in the Cu could not explain the prominent maximum of $M_S(x_{\text{BEP}})$ (Fig. 8) for a limited range of doping levels. Rather, an increasing M_S with increasing x_{BEP} would be expected because the volume of the Cu-Ga (for $x_{\text{BEP}} > 1\%$) as well as the impurity concentration should increase with x_{BEP}. The total magnetic moment arising from magnetic impurities in the source materials or In, for instance Fe with $M_S^{\text{Fe}} = 1.7 \times 10^6$ A/m, is estimated to be $m < 1 \times 10^{-9}$ A m^2 for sample N0335, much smaller than the measured $m = 68 \times 10^{-9}$ A m^2 (cf. Table I). Hence, the reduction of the magnetization by etching in HCl and HNO_3 points to a modification of the film microstructure.

V. DISCUSSION

The magnetization measurements indicate a ferromagnetic behavior of our MBE-grown GaN:Cu films for $x_{\text{BEP}} \approx 1\%$ with small coercivity. Hysteresis loops with small coercivity have been reported earlier for various DMSs.[13,14,16] If the formation of Cu-Ga islands is disregarded and the BEP ratio is taken as the doping level of Cu in GaN, the maximum $M_S = 10.53 \times 10^3$ A/m obtained for sample N0362 with $x_{\text{BEP}} = 1.1\%$ corresponds to a saturation moment of 2.33 μ_B/Cu close to the value predicted by theory.[11] However, the moment decreases with increasing film thickness. Moreover, due to the large amount of Cu-Ga islands on the film surface the true Cu concentration in the GaN host is considerably lower than the nominal doping level x_{BEP}. TEM data indicate a Cu concentration of ≈0.1 at. % and ≈0.04 at. % in the GaN host for metal-rich grown GaN with $x_{\text{BEP}} = 1.2\%$ and 4.8%, respectively.[22] The excess Cu precipitates into Cu-Ga islands at the surface, as discussed above. Hence, the average magnetic moment per Cu atom is about two orders of magnitude larger than 2 μ_B/Cu. This suggests that in a local picture each Cu atom gives rise to a magnetic polarization that extends over tens of lattice constants.

Formation of a colossal moment was reported for Gd-doped GaN and was attributed to a long-range spin polarization of the GaN matrix by the Gd atoms.[8] In that case the continuous increase and saturation of M_S with Gd concentration was explained by a percolation model. In the present case we do not observe a saturation of M_S at high x_{BEP} but long-range ferromagnetic order in a limited range of doping levels corresponding to $x_{\text{BEP}} \approx 1\%$.

The origin of ferromagnetic behavior in Cu-doped GaN has been discussed in theory. Cu could be incorporated in the GaN lattice on Ga sites inducing ferromagnetic behavior by Zener double exchange[28] or *p-d* hybridization mechanism.[29] The latter was suggested by Wu *et al.* to be responsible for the spin polarization in GaN:Cu, where one Ga atom is substituted by Cu at a concentration of 6.25 at. %.[11] However, detailed x-ray absorption studies performed on our films in connection with numerical simulations reveal that only 40% of the Cu atoms are substituted on Ga sites while 55% are at interstitial sites and a minor fraction of 5% on N sites.[20]

The incorporation of interstitial Cu may cause magnetically active lattice defects due to the formation of point defects, voids, and dangling bonds, which may also induce ferromagnetic behavior. A Ga vacancy in GaN induces a local magnetic moment of 0.23–0.29 μ_B/N at the N neighbors.[30] Defects in Cu-implanted GaN were also proposed to induce exchange coupling and long-range ferromagnetic order.[15] Furthermore, in undoped GaN nanoparticles a ferromagnetic magnetization was observed which decreases with increasing particle size possibly due to the decreasing number of Ga vacancies.[31] DFT calculations have shown that Ga vacancies (point defects) in GaN act as acceptors.[32] The charged vacancies exhibit a magnetic moment of 3 μ_B/defect resulting in long-range magnetic coupling due to the extended tails of the defect wave function. In this context, Dev *et al.* argued that doping GaN with Gd gives rise to a strong increase of the defect density well above the density of Gd dopands.[32]

In the present case, the Cu atoms which are incorporated during film growth could aggregate along the threading dislocations which are generated by the heteroepitaxial growth of GaN on AlN and partially fill them.[24] These metal-filled threading dislocations may induce a magnetic polarization in their vicinity. We conclude that with increasing BEP ratio the density of dislocations—aggregated with Cu—increases due to the incorporation of Cu into GaN up to a $x_{\text{BEP}} \approx 1\%$. For $x_{\text{BEP}} > 1\%$ the segregation of Cu to the surface is favored in connection with a reduced defect density in the film. In

addition, the dislocation density decreases with increasing film thickness. This scenario explains the observed concentration and thickness dependence of $M_S(x_{BEP})$ (cf. Fig. 8).

VI. CONCLUSION

Cu-doped GaN films with various Cu concentrations and thicknesses have been grown by MBE. Characterization of the samples shows that only a fraction of Cu provided by the beam is incorporated into the GaN film. For metal-rich and nitrogen-rich grown samples most of the Cu precipitates in the form of nonferromagnetic Cu-Ga islands at the surface. The precipitation increases with increasing Cu-to-Ga BEP ratio x_{BEP}. The Cu-doped GaN films exhibit room-temperature ferromagnetism with a maximum saturation magnetization in a small range of Cu concentration corresponding to $x_{BEP} \approx 1\%$. The ferromagnetic order is presumably induced by defects, mainly threading dislocations, with a density that strongly increases when Cu is supplied by the beam. The role of the defect density is inferred from the decreasing magnetization with increasing film thickness. Our preliminary explanation considers Cu-induced dislocations which give rise to the formation of a magnetic polarization with a magnetic moment per Cu atom much larger than the value of 2 μ_B/Cu predicted by theory. Beyond $x_{BEP} = 1\%$ the defect density decreases due to segregation of Cu to the surface and the depletion of Cu in the film. Consequently, M_S is strongly reduced for $x_{BEP} > 1\%$. An alternative explanation would be a modification of the width of the space charge layer below the surface due to the doping-level dependent charge carrier density. This would be affected by the film thickness, too. Whether such a charge-carrier-induced magnetization occurs will be investigated by future Hall-effect measurements.

ACKNOWLEDGMENTS

This research was partially supported by Project No. A2.7 of the DFG-Center for Functional Nanostructures. We thank Veronika Fritsch for experimental help and Hilbert v. Löhneysen for useful comments.

*christoph.suergers@kit.edu

[1] T. Dietl, H. Ohno, F. Matsukura, J. Cibert, and D. Ferrand, Science **287**, 1019 (2000).

[2] T. Dietl, Nat. Mater. **9**, 965 (2010).

[3] I. Žutić, J. Fabian, and S. Das Sarma, Rev. Mod. Phys. **76**, 323 (2004).

[4] G. M. Dalpian and S. H. Wei, Phys. Rev. B **72**, 115201 (2005).

[5] G. T. Thaler, M. E. Overberg, B. Gila, R. Frazier, C. R. Abernathy, S. J. Pearton, J. S. Lee, S. Y. Lee, Y. D. Park, Z. G. Khim, J. Kim, and F. Ren, Appl. Phys. Lett. **80**, 3964 (2002).

[6] S. Dhar, L. Perez, O. Brandt, A. Trampert, K. H. Ploog, J. Keller, and B. Beschoten, Phys. Rev. B **72**, 245203 (2005).

[7] J. M. Baik, H. W. Jong, J. K. Kim, and J. L. Lee, Appl. Phys. Lett. **82**, 583 (2003).

[8] S. Dhar, O. Brandt, A. Trampert, L. Däweritz, K. J. Friedland, K. H. Ploog, J. Leller, B. Beschoten, and G. Güntherodt, Appl. Phys. Lett. **82**, 2077 (2003).

[9] X. Feng, J. Phys.: Condens. Matter **16**, 4251 (2004).

[10] D. B. Buchholz, R. P. H. Chang, J. H. Song, and J. B. Ketterson, Appl. Phys. Lett. **87**, 082504 (2005).

[11] R. Q. Wu, G. W. Peng, L. Liu, Y. P. Feng, Z. G. Huang, and Q. Y. Wu, Appl. Phys. Lett. **89**, 062505 (2006).

[12] A. L. Rosa and R. Ahuja, Appl. Phys. Lett. **91**, 232109 (2007).

[13] B. Seipel, E. Erni, A. Gupta, C. Li, F. J. Owens, K. V. Rao, N. D. Browning, and P. Moeck, J. Mater. Res. **22**, 1396 (2007).

[14] J.-H. Lee, I.-H. Choi, S. Shin, S. Lee, J. Lee, C. Whang, S.-C. Lee, K.-R. Lee, J.-H. Baek, K. H. Chae, and J. Song, Appl. Phys. Lett. **90**, 032504 (2007).

[15] X. L. Yang, Z. T. Chen, C. D. Wang, Y. Zhang, X. D. Pei, Z. J. Yang, G. Y. Zhang, Z. B. Ding, K. Wang, and S. D. Yao, J. Appl. Phys. **105**, 053910 (2009).

[16] H.-K. Seong, J.-Y. Kim, J.-J. Kim, S.-C. Lee, S.-R. Kim, U. Kim, T.-E. Park, and H.-J. Choi, Nano Lett. **7**, 3366 (2007).

[17] H. J. Xiang and S.-H. Wei, Nano Lett. **8**, 1825 (2008).

[18] C. H. Choi, S. H. Kim, H. J. Lee, Y. H. Jeong, and M. H. Jung, J. Mater. Res. **24**, 1716 (2009).

[19] P. R. Ganz, C. Sürgers, G. Fischer, and D. M. Schaadt, J. Phys. Conf. Ser. **200**, 062006 (2010).

[20] R. Schuber, P. R. Ganz, F. Wilhelm, A. Rogalev, and D. M. Schaadt, Phys. Rev. B **84**, 155206 (2011).

[21] Y. Zhang, J.-B. Liang, J. K. Liang, Q. Zhang, B. J. Sun, Y. G. Xiao, and G. H. Rao, J. Alloys Compd. **438**, 158 (2007).

[22] T.-H. Huang, P. R. Ganz, L. Chang, and D. M. Schaadt, J. Electrochem. Soc. **158**, H860 (2011).

[23] A. R. Smith, D. J. Arnold, and R. W. Mires, Phys. Rev. **2**, 2323 (1970). For conversion from χ_m (cgs units) to χ (SI units) we have used a mass density $\rho = 3.94$ g/cm^3 for Al_2O_3.

[24] J. W. P. Hsu, M. J. Manfra, D. V. Lang, S. Richter, S. N. G. Chu, A. M. Sergent, R. N. Kleiman, and L. N. Pfeiffer, Appl. Phys. Lett. **78**, 1685 (2001).

[25] E. J. Miller, D. M. Schaadt, E. T. Yu, X. L. Sun, L. J. Brillson, P. Waltereit, and J. S. Speck, J. Appl. Phys. **94**, 7611 (2003).

[26] D.-Y. Wang, N. Nakamine, and Y. Hayashi, J. Vac. Sci. Technol. A **16**, 2084 (1998).

[27] E. J. Miller, D. M. Schaadt, E. T. Yu, P. Waltereit, C. Poblenz, and J. S. Speck, Appl. Phys. Lett. **82**, 1293 (2003).

[28] H. Akai, Phys. Rev. Lett. **81**, 3002 (1998).

[29] K. Sato, P. H. Dederichs, H. Katayama-Yoshida, and J. Kudrnovský, J. Phys.: Condens. Matter **16**, S5491 (2004).

[30] J. Hong, J. Appl. Phys. **103**, 063907 (2008).

[31] C. Madhu, A. Sundaresan, and C. N. R. Rao, Phys. Rev. B **77**, 201306 (2008).

[32] P. Dev, Y. Xue, and P. Zhang, Phys. Rev. Lett. **100**, 117204 (2008).